



Plumbagin binds to epidermal growth factor receptor and mitigate the effects of epidermal growth factor micro-environment in PANC-1 cells

Loganayaki Periyasamy¹ · Bharathi Murugantham² · Sridhar Muthusami^{1,2}

Received: 24 March 2023 / Accepted: 5 May 2023 / Published online: 20 May 2023

© The Author(s), under exclusive licence to Springer Science+Business Media, LLC, part of Springer Nature 2023

Abstract

A sustained increase in the mortality of pancreatic cancer (PC) and sudden metastasis-related mortality is a cause for concern. Aberrant expression of epidermal growth factor (EGF) receptor (EGFR) is noted in several cases of PC metastasis. The present study is aimed at analyzing the expression of EGFR in PC and its relevance to the progression of PC. Despite the number of studies that have shown the benefits of plumbagin on PC cells, its role on cancer stem cells remains largely unknown. To this end, the study used an EGF micro-environment to make cancer stem cells in vitro and ascertained the role of plumbagin in mitigating the actions of EGF. The Kaplan–Meier (KM) plot indicated reduced overall survival (OS) analysis in PC patients with high EGFR than low EGFR expression. Plumbagin pre-treatment significantly prevented EGF-induced survival, epithelial-to-mesenchymal transition (EMT), clonogenesis, migration, matrix metalloproteinase -2 (MMP-2) gene expression and its secretion, and matrix protein hyaluron production in PANC-1 cells. The computational studies indicate the greater affinity of plumbagin with different domains of EGFR than gefitinib. Several hallmarks of resistance and migration due to EGF are effectively attenuated by plumbagin. Collectively, these results warrant investigating the actions of plumbagin in a pre-clinical study to substantiate these findings.

Keywords Pancreatic cancer · EGFR · Migration · Plumbagin · MMP-2

Abbreviations

PC	Pancreatic cancer	ELISA	Enzyme-linked immunosorbent assay
EGFR	Epidermal growth factor receptor	PanIN	Pancreatic intraepithelial neoplasia
KM	Kaplan–Meier	PBS	Phosphate buffered Saline
SDF	Structural data file	PDAC	Pancreatic ductal adenocarcinoma
OS	Overall survival	PFS	Progression-free survival
RCSB	Research collaboratory for structural bioinformatics, PDB: Protein data bank	STAT 3	Signal transducer and activator of transcription 3
EMT	Epithelial-to-mesenchymal transition	NF-κB	Nuclear factor kappa light chain enhancer of activated B cells
MMP-2	Matrix metalloproteinase -2	TGCA	The cancer genome atlas
ICMR	Ndian council of medical research	GEPIA	Gene expression profiling interactive analysis
TME	Tumor microenvironment	UALCAN	University of ALabama at Birmingham CANcer data analysis portal
TGF-β	Transforming growth factor- beta	NCCS	National center of cell sciences
KRAS	Kirsten rat sarcoma	MTT	3-(4,5-Dimethylthiazol-2-yl)-2,5-Diphenyltetrazolium Bromide
		PI	Propidium iodide
		AO	Acridine orange
		EtBr	Ethidium bromide
		RT-PCR	Reverse transcription-polymerase chain reaction
		TM	Transmembrane

✉ Sridhar Muthusami
sridharuniv@gmail.com; sridhar.m@kahedu.edu.in

¹ Department of Biochemistry, Karpagam Academy of Higher Education, Coimbatore 641021, Tamil Nadu, India

² Karpagam Cancer Research Centre, Karpagam Academy of Higher Education, Coimbatore 641021, Tamil Nadu, India

JM	Juxta membrane
TK	Tyrosine kinase
RU	Regulatory unit
ANOVA	Analysis of variance
CD	Cluster of differentiation

Introduction

The occurrence of PC is constantly increasing only with marginal improvement in the patient's survival. The development of resistance to various treatments such as surgery, chemotherapy, and radiation is a major cause of concern [1]. Less than 20% of PC subjects are eligible to undergo surgical removal of tumors, moreover, the complex interplay of the tumor with the superior mesenteric/hepatic blood arteries restricts the operative feasibility [2]. GLOBOCAN, (2020) reported 466,000 mortalities among 496,000 PC patients. In India, PC incidence is ranked 21st in males and 17th in females [3]. Indian council of medical research (ICMR) approved approaches for diagnosis includes histopathological confirmation, staging based on tumor, and lymph node metastasis. For the management of PC, a first-line treatment using gemcitabine is prescribed along with nab-paclitaxel and FOLFIRINOX. In non-responsive individuals, curative resection is performed, and encouraged to participate in clinical trials for newer metastasis prevention drugs [4]. The presence of growth factors in the tumor microenvironment (TME) is identified as a causal factor for the metastasis of several cancers [5]. Epithelial-to-mesenchymal transition (EMT) is regarded as a key event for the initiation of metastasis by enriching the mesenchymal genotypes and phenotypes in PC. Epidermal growth factor (EGF), transforming growth factor- beta (TGF- β), and other growth factors are well-known to promote metastasis [6]. Several findings demonstrated the vital role of EGF in fostering PC metastasis [7]. EGF receptor (EGFR) amplification and Kirsten rat sarcoma (KRAS) mutations are regarded as early events for the development of PC [8]. EGFR expression is undetectable in the normal pancreatic tissue during the initial neoplastic changes such as pancreatic intraepithelial neoplasia (PanIN)1A and PanIN-1B. A gradual increase in EGFR is noted in PanIN 2, PanIN 3, and pancreatic ductal adenocarcinoma (PDAC) [9]. Studies from our laboratory and others have shown the significance of EGFR signaling in many cancers including PC [10–12]. Further, one-third of PC individuals with EGFR overexpression developed lymph node metastasis [13]. A large population (30–89%) of individuals diagnosed with PC displays an abundance of EGFR overexpression in the TME [14]. A meta-analysis study revealed that treatment of PC with a combination of gemcitabine and erlotinib showed improvement in PC OS

and progression-free survival (PFS), though with various adverse side effects [15]. Therefore, the development of EGFR inhibitory molecules with less or no side effects would potentially benefit PC patients with high EGFR expression. A recent study from our laboratory delineated the significance of phyto components in exerting anti-metastasis activity against PC progression [16]. There is a need to identify naturally existing novel phyto-constituents to circumvent the sustenance and metastasis of PC. Preliminary screening conducted using cell-based and computational approaches using various phytocomponents identified plumbagin to be effective at lower concentrations [17]. Plumbagin, an active ingredient of *Plumbago zeylanica* exerts anti-cancer activity in various cancers including PC, and its dose- and time-dependently suppress PC cell proliferation. Targeting the signal transducer and activator of transcription 3 (STAT3), EGFR, and nuclear factor kappa light chain enhancer of activated B cells (NF- κ B) signaling pathways, plumbagin treatment promotes apoptosis and reduces cell viability both in vitro and in vivo [18]. Although the anti-cancer effect on PC has been assessed, studies substantiating the effect of plumbagin under EGF-driven PC are unknown. Therefore, the proposed study is determined at exploring the relevance of EGFR overexpression in PC and the ability of plumbagin in mitigating EGF actions in vitro.

Materials and methods

Analysis and validation of EGFR expression in PC

The EGFR expression pattern in PC patients was retrieved from the cancer genome atlas (TCGA) and analyzed using gene expression profiling interactive analysis (GEPIA) (<http://gepia.cancer-pku.cn/>) tool with the cutoff of $|\text{Log}_2\text{FC}| = 1.0$ and $p\text{-value} = 0.05$. The TCGA sample size for the normal is 171 and the PC tumor is 179. EGFR expression was analyzed in the PC major stages with the probability of fold value ($\text{Pr}(> F)$) [19]. Likely, the EGFR expression was compared based on the age group using the University of ALabama at Birmingham CANcer data analysis portal (UALCAN) server (<http://ualcan.path.uab.edu>). UALCAN is a database for studying cancer transcriptome data that can be accessed online. Overall survival (OS) of individuals with high EGFR was determined to validate the rationale behind targeting EGFR inhibitors.

The OS survival analysis

The patient survival probability of EGFR was assessed using a Kaplan–Meier (KM) survival chart, with a log-rank

P-value of 0.05 obtained by GEPIA2, and the TCGA patient dataset were divided into two halves (high versus low expression) [19]. The probability of survival was calculated using, $\hat{S}(t) = \prod_{i: t_i \leq t} \left(1 - \frac{d_i}{n_i}\right)$,

Where t is the moment in time when an incident occurred, d_i is the total number of events that took place at time t, and n_i is the total number of survivors up to time t.

Culturing and maintenance of cell line

Human PC cell line PANC-1 was obtained from the national center of cell sciences (NCCS), (Pune, India) and cultured in DMEM medium with 10% of FBS, 1% of the antibiotic, and antimycotic solution. The cells were maintained in 5% CO₂ at 37 °C in a humidified atmosphere (Thermo scientific, BB150). Upon confluence, the cells were trypsinized and the detached cells were used either for culturing or for experimental analysis.

Cell viability assay

To determine the dose-dependent activity of plumbagin, the cells were treated with 2 μM, 4 μM, 6 μM, 8 μM, and 10 μM of plumbagin for 24 h, respectively. To ascertain the effect of plumbagin on PANC-1 cell viability in basal and stimulation with EGF, the cells were treated with plumbagin (5 μM) and EGF (50 ng/ml) for 24 h. Plumbagin (5 μM) treatment for 30 min before EGF (50 ng/ml) stimulation. The untreated cells in a serum-free medium served as control. After 24 h, 3-(4,5-Dimethylthiazol-2-yl)-2,5-Diphenyltetrazolium Bromide (MTT) solution (0.5 mg/ml) was prepared in the dark and replaced for media for 3 h to assess mitochondrial functioning, which is indicated by the formazan crystals generated. For quantification, these crystals were solubilized using an organic solvent and read at 520 nm in an enzyme-linked immunosorbent assay (ELISA) reader (BioTek, Synergy H1). A graphical chart was attained by plotting absorbance vs concentration of plumbagin and has been used to calculate the percentage viability.

Cell cycle arrest

PANC-1 cells were cultured in six-well plates and treatment was carried out as mentioned in Sect. “Cell viability assay”. After 24 h of treatment, the cells were subjected to trypsinization, phosphate buffered saline (PBS) wash was given twice, and placed in a solution containing propidium iodide (PI), an intercalating agent for 30 min at 37 °C. Distribution of cell cycle phases determined by flow cytometer to

understand the role of plumbagin and EGF on the cell cycle (Beckman Coulter—DxFLEX).

Acridine orange (AO)/Ethidium bromide (EtBr) staining

The culturing and drug treatment were followed as mentioned in Sect. “Cell viability assay”. After 24 h of treatment, the cells were stained with AO (100 μg/ml) and EtBr (100 μg/ml) and the excessive stain were washed out using PBS. The cells were analyzed and captured using a fluorescent microscope (ZOE™ Fluorescent Cell Imager, BioRad).

Assessment of EMT

The culturing and treatment were followed as mentioned in Sect. “Cell viability assay”. After 24 h of treatment, the cellular morphology was assessed using microscopic analysis to identify EMT. The captured photomicrographs indicating the spheroid to spindle morphology were captured and represented in Fig. 3.

RNA extraction and real-time reverse transcription-polymerase chain reaction (RT-PCR)

RNA extracted from treated and untreated PANC-1 cells using the Trizol reagent. cDNA synthesis was carried out using 2 μg of isolated RNA with reverse transcriptase enzyme (GBiosciences). Real-time PCR was used to quantify the expression of the matrix metalloproteinase- 2 (MMP-2) gene using the EvaGreen qPCR Master Mix. Briefly, the reaction mixture contains 2X 10 μl of master mix, 2 μl of template cDNA, 2 μl of both forward and reverse primer for MMP-2 (primer sequence given below), and 4 μl of nuclease-free water. The cycle program includes denaturation for 10 s at 95 °C (45 cycles), annealing for 10 s at 55 °C, and extension for 10 s at 72 °C followed by the activation of enzymes (95 °C) for 2 min. MMP-2 and β-actin transcripts were relatively quantified using $2^{-\Delta\Delta CT}$.

Gene	Forward primer	Reverse primer
β-actin	5’GACAGG	5’TGATCC
	ATGCAG	ACATCT
	AAGGAG	GCTGGA
	ATCACT3’	AGGT3’
MMP-2	5’GATACC	5’CCTTCT
	CCTTTG	CCCAAG
	ACGGTA	GTCCAT
	AGGA3’	AGC3’

Gelatin zymography

The treatment was followed as outlined in Sect. “[Cell viability assay](#)”, and the conditioned medium was aspirated and centrifuged to eliminate debris. An equal quantity of proteins from different groups was electro-separated in a gelatin-embedded SDS-PAGE to recover the tertiary structure of the protein, and the gel was immersed in a renaturation buffer for 24 h. Incorporated gelatin has been digested by active MMPs and to find areas of degradation, which are shown by a white band against a blue background, a coomassie stain was used. The Chemidoc, Biorad documentation was utilized to capture the intensity of achromatic bands and represented as a high-resolution image file.

Cell migration assay

Briefly, the cells upon reaching confluence, a wound was created using a 20–200 μ l pipette tip, and rinsed in PBS to get rid of the detached cells. Then, EGF (50 ng/ml), plumbagin (5 μ M), and plumbagin pre-treatment (30 min) are given followed by EGF stimulation for the indicated time point. As a control, a serum-free medium was used. Photomicrographs were taken at 0 h, 12 h, 24 h, and 36 h to compare the wound healing between the treated and untreated groups. To assess the migration pattern of treated cells, the unclosed wound areas were measured at different time points.

Colony formation assay

PANC-1 cells were cultured in a 6-well plate using DMEM media and maintained in a 5% CO₂ atmosphere at 37 °C. Plumbagin pre-treatment (30 min) was given to two sets of groups. After 30 min, one group was stimulated with EGF and the other group was left as such. Serum-free media-treated cells were used as control. After 24 h of treatment, the drug-containing media was removed and maintained with 2% FBS for 14 days. The cells were rinsed with PBS and crystal violet was used to stain to compare the colony growth between the treated and untreated groups.

Assessment of hyaluron production

The treatment was carried out in line with Sect. “[Cell viability assay](#)” description. The cells were treated for 24 h before being rinsed with PBS and fixed with 2% glacial acetic acid in ethanol. Afterward, rinse with 95% and 70% ethanol for 5 min. The cells were then fixed, stained with alcian blue (pH 2.5) in 0.1 N HCL for an overnight period, then rinsed with 0.1 N HCL to remove unbound dye. The bounded dye was dissolved in guanidine-HCL and measured colorimetrically at 630 nm.

Molecular docking

The 3D structure of gefitinib and plumbagin were obtained from the database of PubChem compounds (<https://pubchem.ncbi.nlm.nih.gov>) and saved in the structural data file (SDF) file format. The EGFR domains were generated by retrieving EGFR complex with a co-crystallized ligand from the Research Collaboratory for Structural Bioinformatics (RCSB) Protein Data Bank (PDB) for domains 1 and 2 (1dnq), domains 2 and 3 (1dnr), Transmembrane (TM) and Juxta membrane (JM) (2n5s), and tyrosine kinase (TK) and regulatory (RU) (6duk). The EGFR domain PDB files were modified using the Discovery Studio Visualizer v19.1.0.18287 to eliminate unwanted bounded ligands and molecules of water before being exported in PDB format. The force field was set at off on PyRx to obtain atomic coordinates and reduce energy for the stored SDF format of the ligand, which was afterward changed into PDBQT format [20]. The PyRx tool with the option Aurodock Vina v1.1.2 for docking was used to convert modified EGFR domains in PDB format into PDBQT files [21, 22]. PyRx was included with Autodock Vina utilizing the new scoring function after preparing receptors and ligands [21]. Size $x = 89.2949453291$, Size $y = 130.660572357$, and Size $z = 70.5163963609$ were fixed for the grid box dimensions, and they were docked with the EGFR.

Statistical analysis

The statistical analysis used in this study utilized analysis of variance (ANOVA) to investigate the obtained numerical data. To determine the differences between the individual groups using the numerical information obtained from at least three independent replicates, the student “t” test was employed. If the $p < 0.05$, it is deemed statistically significant.

Results

EGFR expression based on PC samples and ages, OS survival analysis, and stage plot

The EGFR expression was upregulated in the PC-affected patients’ samples without statistical significance ($P \leq 0.05$) (Fig. 1A). However, the increased EGFR expression was reducing the patient’s survival rate severely ($p = 0.029$) (Fig. 1B). Also, EGFR expression was examined at major stages of PC from the TCGA database. The EGFR was significantly distributed stage-wide with higher expression in tumor stage II (highlighted in red) (Fig. 1C). The EGFR expression in different age groups viz, > 20 (Median (M) = 5.515), 21–40 years ($M = 10.64$), 41–60 years

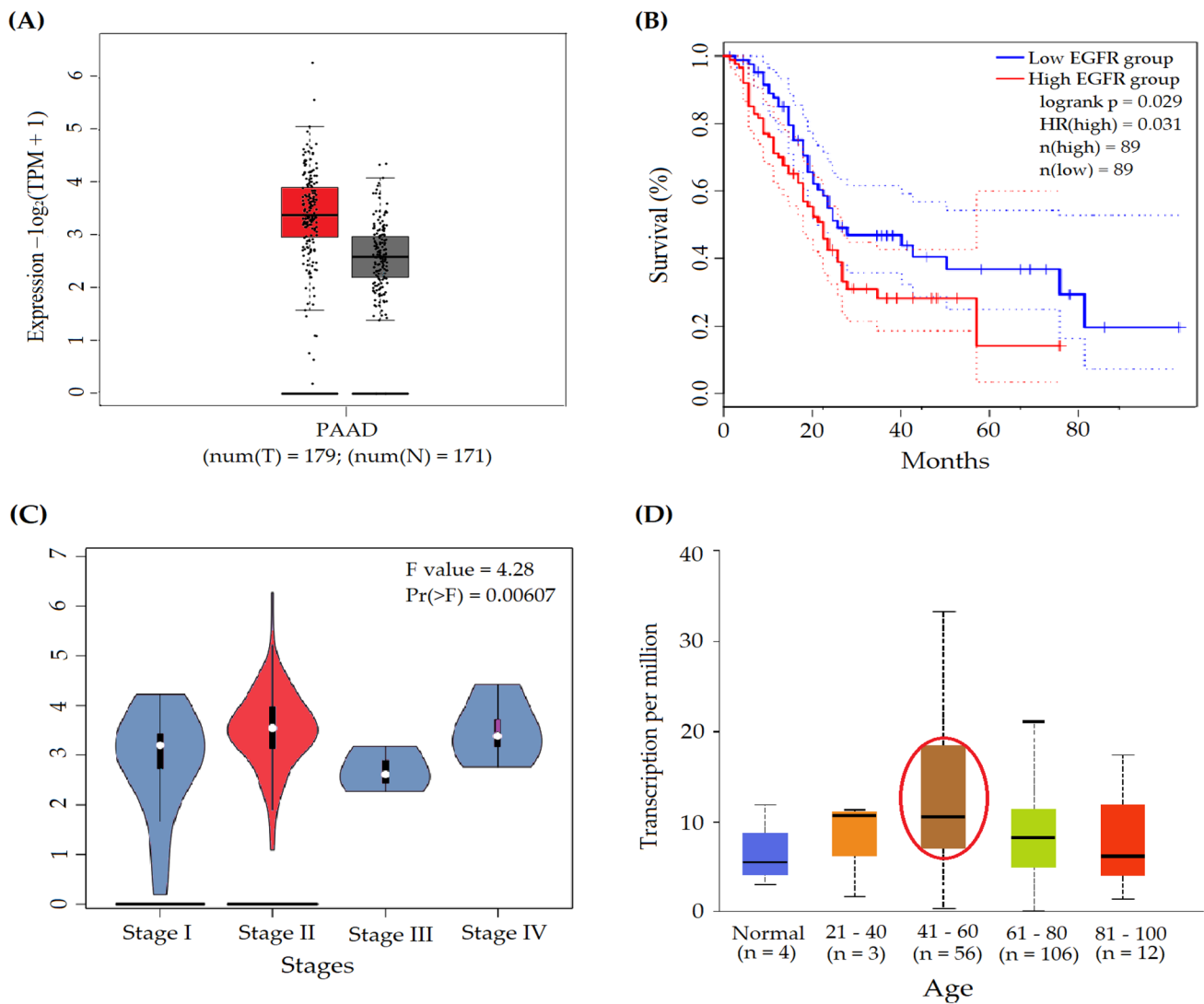


Fig. 1 Depicts the relevance of EGFR expression in PC and adjacent normal tissues, the OS analysis, and the stage plot for PC cancer patients. **A** EGFR expression rate **(B)** OS rate **(C)** EGFR expression based on age group **(D)** The association between EGFR expression

and PC stages as analyzed by stage plot along with analysis of variance (ANOVA). The level of statistical significance (*F*) at the probability (*p*) value is indicated in the plot

(*M* = 10.613), 61–80 years (*M* = 8.146), 81–100 years (*M* = 6.12) group were analyzed. The number of patients affected by PC was higher in the age group between 41–80 years (*p* = 0.000918). Even though, the EGFR expression was increased at the age group of 41–60 years based on the predicted media value (Fig. 1D).

Effects of plumbagin on cell viability, cell cycle analysis and apoptosis

To determine the viability after treatment, PANC-1 cells were exposed to various concentrations (2 μM– 10 μM) for 24 h. The photomicrographs of the plumbagin-treated cells displayed evidence of cell detachment, blebbing, shrinkage

of cells, and cellular fragmentation (Fig. 2A). In a concentration-dependent manner, plumbagin inhibits the survival of PANC-1 cells. Plumbagin at a 6.7 μM dose significantly lowered 50% of viable PANC-1 cells (Fig. 2B). The IC50 value of plumbagin was determined from these data as 6.7 μM in PANC-1 cells. These results are consistent with our recent studies [17].

The treated cells were subsequently analyzed using flow cytometry to assess the role of plumbagin on the distribution of the cell cycle. Plumbagin (5 μM), EGF (50 ng/ml), and a 30 min pre-treatment with plumbagin and EGF stimulation were given as treatment for 24 h. The distribution of cells in the S and G2 phases during the cell cycle for the control group was 22.08% and 35.90%, respectively.

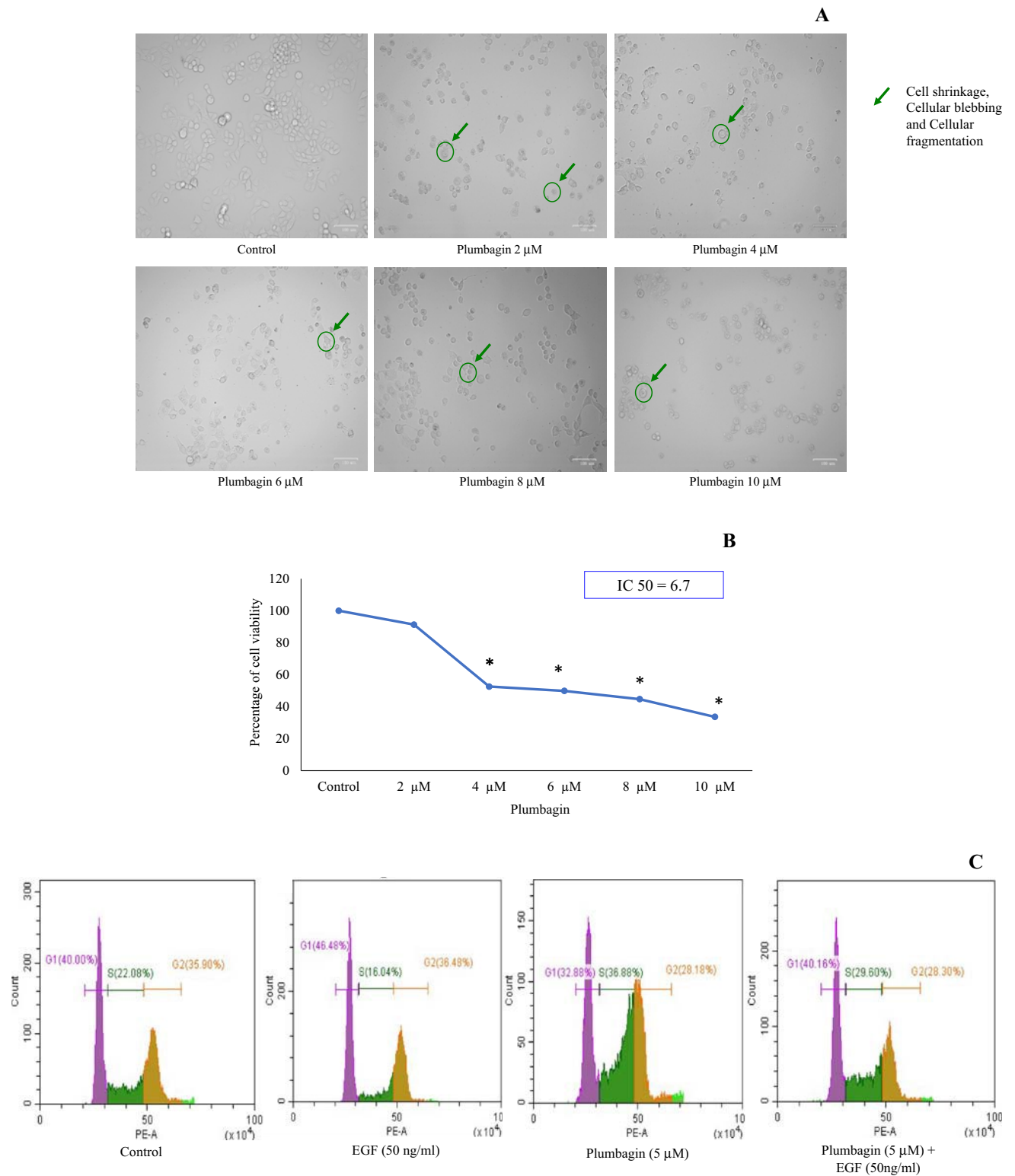


Fig. 2 Human PC PANC-1 cells treated with different (2- 10 μ M) concentrations of plumbagin for 24 h, the photomicrographs were depicted (A) Quantification of cell survival by MTT assay (B). The effect of plumbagin on the distribution of cell cycle after 24 h of treatment was assessed by flow cytometry in basal and EGF-stimu-

lated cells shown in (C). The induction of early and late apoptosis was assessed using AO/EtBr staining after being treated with plumbagin under basal and EGF-stimulated PANC-1 cells for 24 h. * Indicates statistical significance at $p < 0.05$ level

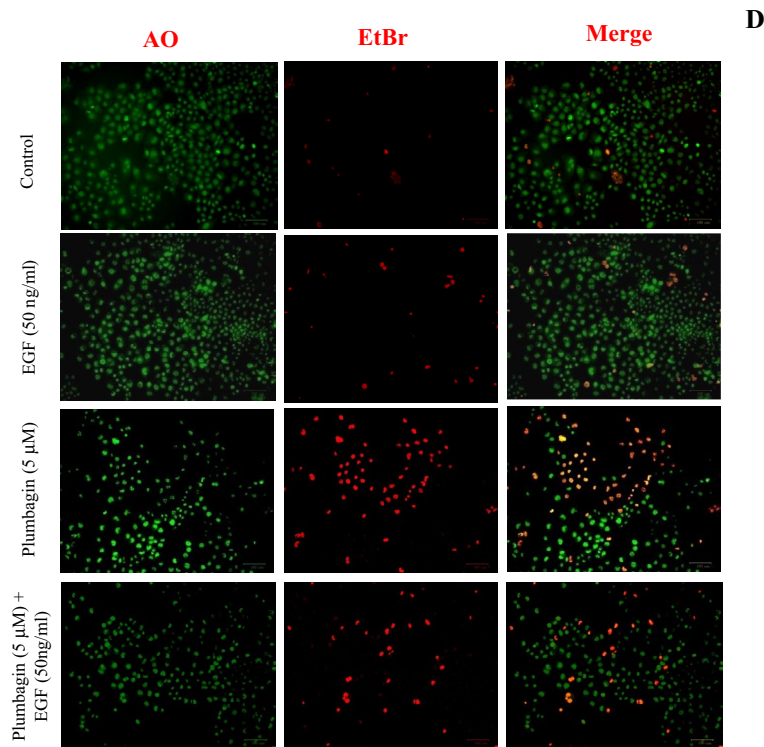


Fig. 2 (continued)

In the S phase and G2 phase, the cells arrested in EGF-treated cells were 16.04 and 35.90, respectively. While plumbagin and plumbagin pre-treatment with EGF-stimulated cells showed 36.88%, 29.60% of the S phase, and 28.18%, 28.30% of the G2 phase respectively, (Fig. 2C). These results suggested that more cells were arrested in the S phase in the plumbagin-treated group (36.88%) when compared to the control (22.08%). Interestingly, plumbagin pre-treatment for 30 min arrested most of the cells in the S phase (29.60%) as compared to EGF-treated cells (16.04%). PANC-1 cells treated with or without EGF were observed to have a normal green nucleus. The dense green and yellow nucleus with chromatin fragmentation indicating early apoptosis and condensed orange chromatin indicating late apoptosis was observed in plumbagin-treated cells under basal and EGF-stimulated PANC-1 cells (Fig. 2D).

Effects of plumbagin on EGF-induced viability, EMT, MMP-2 gene expression, and secretion

PANC-1 cells treated with 50 ng/ml EGF for 24 h demonstrated EMT. The morphological findings showed that EGF-treated cells underwent the spheroid to spindle-shaped cell transformation indicating the onset of EMT. The EMT that was driven by EGF in PANC-1 cells was prevented by plumbagin pre-treatment (Fig. 3A). This data implies that

plumbagin is effective in preventing EGF-induced EMT, which could be attributed to its ability to prevent PC cell migration and metastasis. Further, to understand the effect of plumbagin on viability in both basal and EGF-stimulated conditions, a cell viability assay was performed. Plumbagin at 5 μM concentration drastically reduces the viability after 24 h of treatment. EGF-treated cells significantly increase the number of viable cells when compared to control cells. However, plumbagin 30 min pre-treated cells reduced the EGF-induced survival of PANC-1 cells when compared to EGF-alone treated cells (Fig. 3B).

To ascertain the role of plumbagin in regulating the expression of MMP-2 under basal and EGF-stimulated conditions, RT-PCR was performed. The EGF- treated cells significantly upregulated the MMP-2 gene by 35% when compared to the control cells. Plumbagin treatment significantly downregulates the MMP-2 expression in PANC-1 cells under both basal and EGF- stimulated conditions (Fig. 3D). Simultaneously, the conditioned media from the treated and untreated cells were collected and subjected to gelatin zymography to determine the extracellular secretion and activities of MMP-2. The activity of enzymes is determined using the ability of MMP-2 to digest gelatin embedded in the gel which is visualized as the appearance of a white band against a coomassie blue-stained background. The cells treated with EGF greatly increased the secretion of MMP-2 when compared to untreated control cells in the conditioned

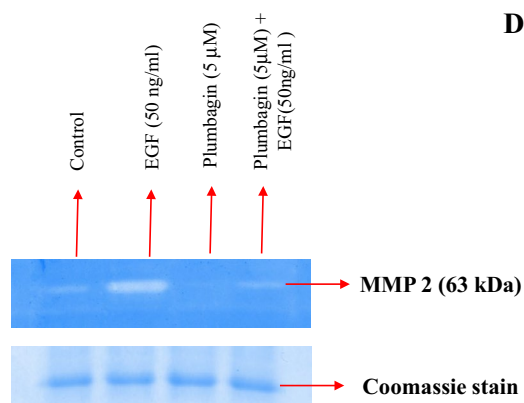
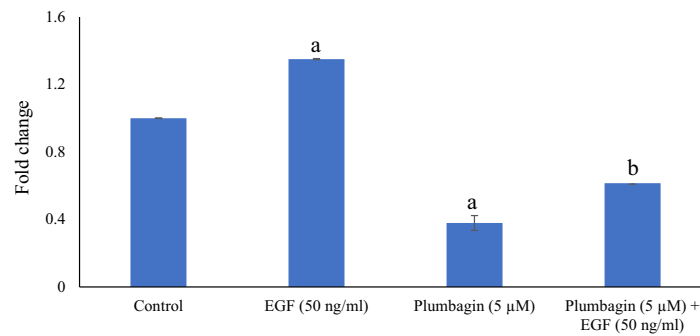
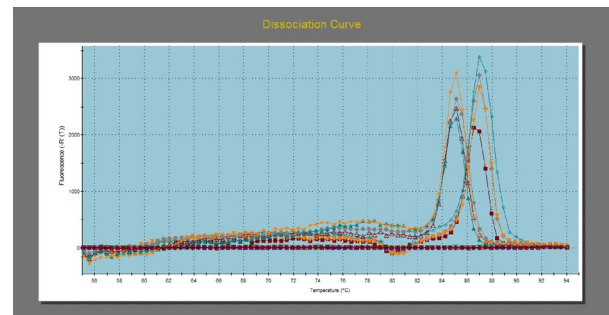
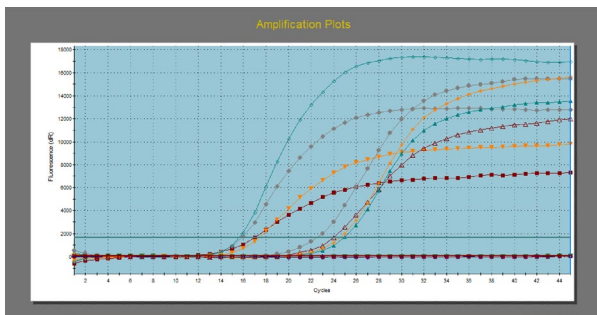
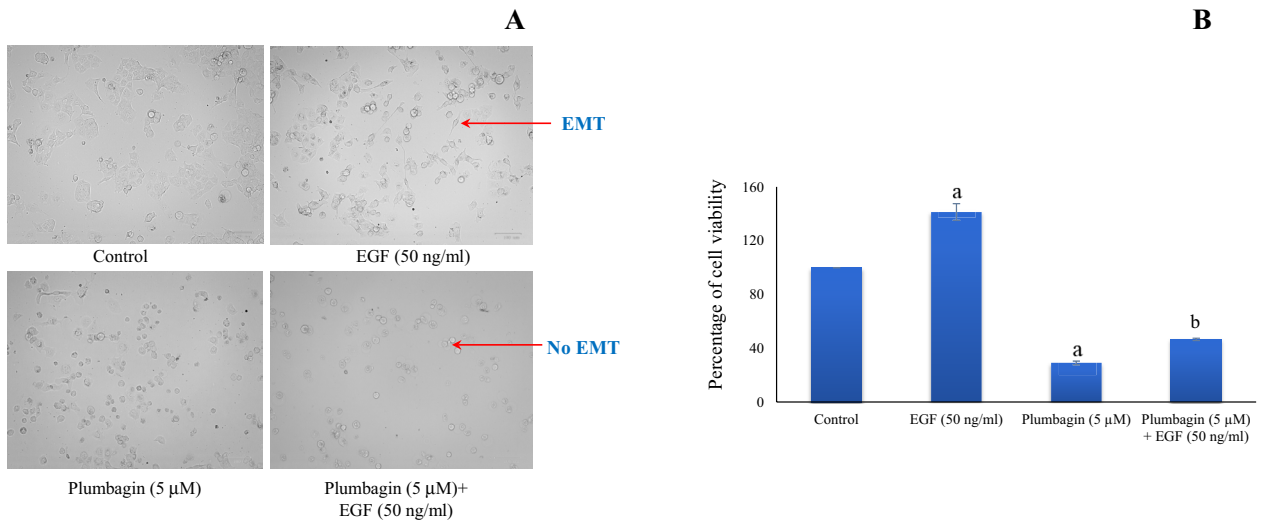


Fig. 3 PANC-1 cells stimulated with EGF promoted the EMT and plumbagin pre-treatment for 30 min prevents EGF-induced EMT (A). The PANC-1 cell survival was assessed after 24 h treatment with EGF in basal and plumbagin pre-treated cells using MTT assay (B). The MMP-2 gene expression was assessed using real-time PCR in the PANC1 cells (C); the conditioned media was used for the evaluation of MMP-2 enzyme activity using gelatin zymography (D). ‘a’—indicates statistical significance ($p < 0.05$) when compared with control. ‘b’—indicates statistical significance when compared with EGF-treated cells

media after 24 h of treatment. Plumbagin treatment effectively blocked the secretion of MMP-2 in the conditioned media of PANC-1 cells under basal and EGF-stimulated cells (Fig. 3E). The activities of MMP-2 are associated with a concomitant increase in the MMP-2 gene expression, indicating that plumbagin interferes with the transcriptional activation of MMP-2 by EGF. Together, these results suggest an important role for plumbagin in inhibiting the EGF-induced survival, EMT, MMP-2 gene expression, and secretion in PANC-1 cells.

Effects of plumbagin on EGF-induced cell migration, colony formation, and hyaluron production

Cell migration is a crucial process involved in several events including cancer cell invasion and metastasis. To assess the efficacy of plumbagin on the PANC-1 cell migration, a wound healing assay was performed. A wound was created and photomicrographs were taken. The area of the wound is measured using image J software. After 12–36 h the wound area was captured to assess the ability of EGF in enhancing the PANC-1 migration and plumbagin to prevent the EGF-induced migration. The migration and repopulation in the scratched area were significantly increased in the EGF-treated cells when compared with control cells (Fig. 4A). Plumbagin treatment potentially reduced the PANC-1 cell migration by 73%, 65%, and 55% for 12, 24, and 36 h, respectively. Similarly, Plumbagin pre-treatment for 30 min effectively retarded the EGF-induced migration in PANC-1 cells by 69%, 60%, and 50% for 12, 24, and 36 h, respectively (Fig. 4B). The EGF-induced EMT and increased secretion of MMP-2 could be attributed as a reason for the increased migration of PANC-1 cells. These effects are not obvious in the cells pre-treated with plumbagin for 30 min suggesting the blockade of EGF-induced wound healing process, indicating the potential therapeutic benefits of plumbagin.

To corroborate the migration studies, we sought to determine the ability of plumbagin to interfere with the propensity of a cell to become a clone, a hallmark of cancer stem cells. To address this, the colony-forming ability of PANC-1 cells treated with EGF and plumbagin was determined by clonogenic assay. 14 days were allowed for the treated and

untreated cells to establish colonies. EGF stimulation has promoted the number of colonies after 14 days, indicating the ability of EGF to induce stemness, a condition reported during tumor relapse. Interestingly, plumbagin pre-treatment abrogated the colony-forming ability, further adding potential therapeutic properties along with reduced EMT and migration (Fig. 4C and D).

The abundance of hyaluron production by EGF in PANC-1 cells indicates the possibility of preventing access to drugs in the EGF-rich TME. This could be a potential reason for the resistance to several drugs. In order to ascertain the role of plumbagin in regulating the non-collagenous matrix component, which contributes to reduced drug access to the tumor site, we performed alcian blue staining to demonstrate the role of plumbagin on the synthesis of hyaluron, a glycosaminoglycan, in PANC-1 cells. Plumbagin treatment decreased the production of hyaluron under basal and EGF-treated cells (Fig. 4E and F).

Molecular docking analysis of EGFR domains and plumbagin

To understand the molecular interaction between plumbagin with different domains of EGFR, we utilized docking experiments. The EGFR structure is composed of six units such as domain I, domain II, domain III, domain IV, TM-JM domain, TK, and RU as depicted in Fig. 5A. The efficacy of plumbagin was compared with the standard drug gefitinib a well-tolerated and orally prescribed EGFR-TK inhibitor. The docked-complex structure of EGFR domains I and II was represented in Fig. 5B. The standard drug gefitinib established the hydrogen bond interaction with the aminoacids ARG84, CYS240, ASP279, and PHE230 residues established an alkyl interaction with -6.0 kcal/mol of binding affinity and 14.378 of RMSD. Further, plumbagin interacted strongly with the ASN70 and TYR101 with -5.7 kcal/mol of binding affinity and 1.342 Å of RMSD. The docked-complex structure of EGFR domains III and IV was represented in Fig. 5C. Interaction of plumbagin with amino acids located in domain III and IV indicate that plumbagin competes with EGF ligand and prevent ligand-receptor interaction. The mode of action of plumbagin appears to be similar to gefitinib, however, the amino acids visualized were different. The standard drug gefitinib established the hydrogen bond and fluorine interaction with ARG390, and LEU363. Also, the alkyl interaction with HIS359, PRO361, PRO365, and LEU368 residues with -5.7 kcal/mol of binding affinity and 3.787 Å of RMSD. Likewise, the plumbagin interacted strongly with ARG427, and ARG509 by hydrogen bond and interact with the residue LYS430 by pi-cation bond. Also, plumbagin formed the pi-alkyl interaction with LYS430 with -6.0 kcal/mol of binding affinity and 2.107 Å of RMSD. The docked-complex structure of TMJM was represented in

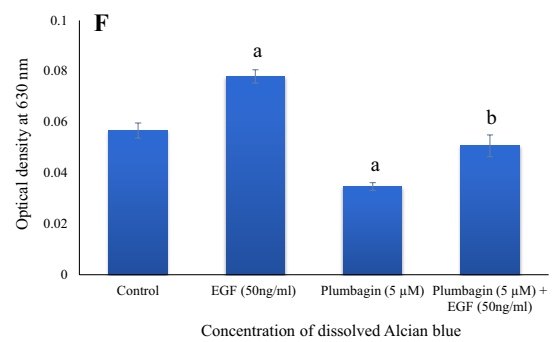
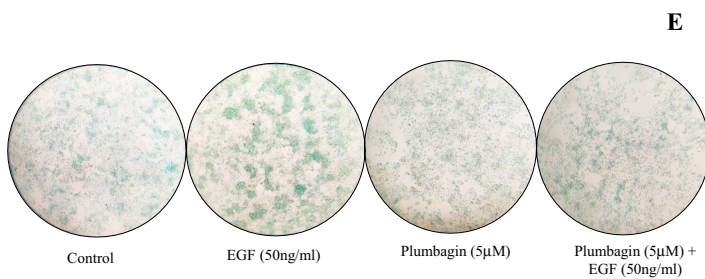
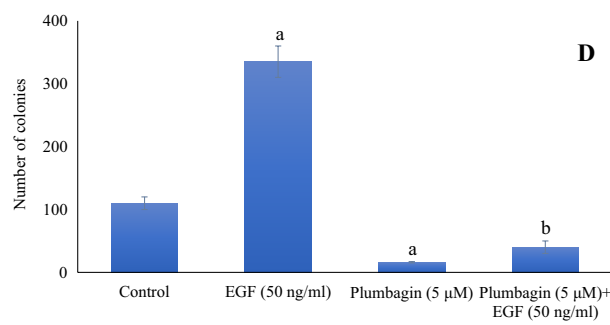
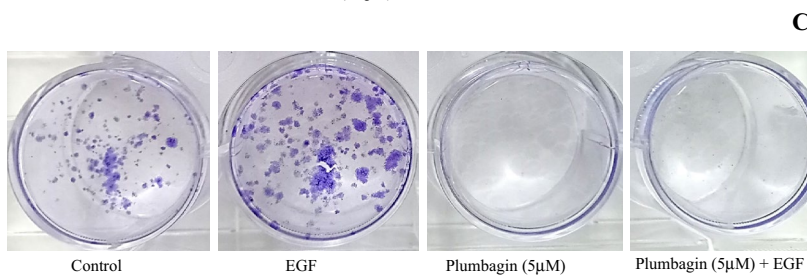
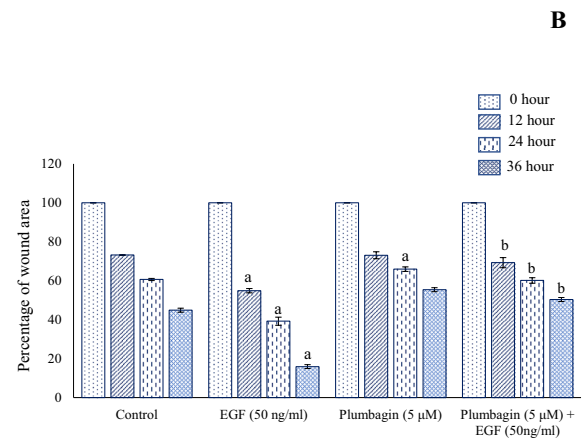
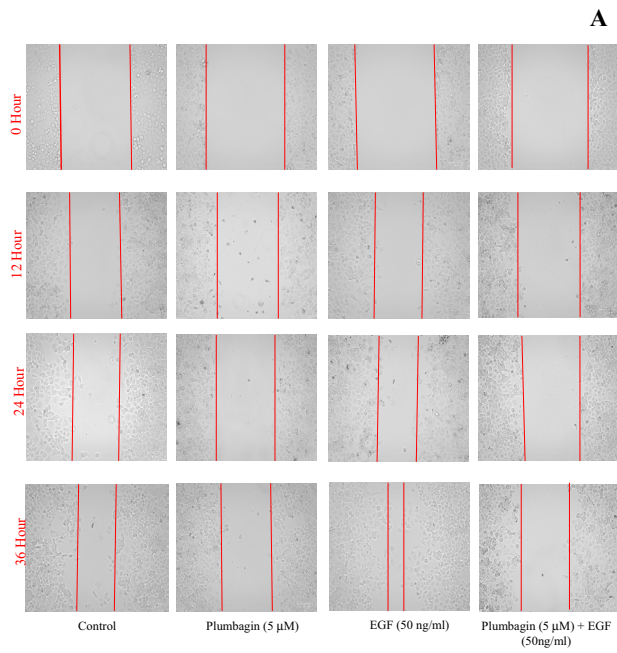


Fig. 4 Photomicrograph shows the ability of cells to migrate in the wound area in different groups at indicated time points 12, 24, and 36 h (**A**). The percentage of the non-occupied area was calculated as an index of relative migration of PANC-1 cells and was measured using Image J software and shown in graph (**B**). The colony formation assay was performed in PANC-1 cells after 24 h of treatment and allowed them to form colonies for 14 days (**C**). The colonies formed were counted and represented in graphical form (**D**). Photomicrographs showing hyaluron production were determined and captured using alcian blue (pH-2.5) staining (**E**) and quantified (**F**). 'a'—indicates statistical significance ($p < 0.05$) when compared with control. 'b'—indicates statistical significance when compared with EGF-treated cells

Fig. 5. D. The standard drug gefitinib formed the alkyl interaction with ARG80 residues with -5.3 kcal/mol of binding affinity and 2.093 Å of RMSD. Likewise, the plumbagin interacted strongly with HIS72 by carbon-hydrogen bond and interacted with the residue LEU79 by Pi-sigma bond. A pi-alkyl interaction with VAL74, LYS76, and LEU79 residues with -4.5 kcal/mol of binding affinity and 1.628 Å of RMSD. The docked-complex structure of TK RU was represented in Fig. 5. E. The standard drug gefitinib formed the carbon-hydrogen bond with MET790 and also bonded with LEU707, PRO733, ILE740, VAL742, and ILE789 by pi-alkyl interaction with -6.4 kcal/mol of binding affinity, 6.758 Å of RMSD. However, the plumbagin strongly interacted with the residues LYS745 and ASP855 by a hydrogen bond. It also extends its pi-sigma interaction with the residues LEU747, LEU788, and LEU858 and pi-alkyl interaction with ILE759, ALA763, and MET766. The predicted binding energy was -7.0 kcal/mol, RMSD 3.621 Å. These results clearly describe the ability of plumbagin to strongly bind with different domains of EGFR than gefitinib as assessed by binding energy and RMSD than gefitinib.

Discussion

PC is reported as an aggressive solid malignancy due to its heterogeneity. The stromal-rich milieu facilitates PC progression and metastasis via the involvement of various growth factors mainly EGF. The reason for the poor therapeutic outcome for PC is mainly due to enhanced metastasis and relapse after surgical resection. Both of these features involve stemness due to a growth factor-rich micro-environment. In this study, we have created this tumor micro-environment to assess the features of metastasis and stemness. In the EGF-rich environment, cells undergo proliferation as well as differentiation as mesenchymal cells. The natural characteristic of mesenchymal cells is to produce several extracellular matrix (ECM) proteins collagenous/non-collagenous to advance the migration and invasion of cancer cells leading to metastasis. Several studies emphasize that EGFR overexpression is associated with poor prognosis

and metastasis and influences the survival of PC patients. The importance of EGFR expression in PC was analyzed using the *in silico* tools. The outcome of the computational experiments supported the hypothesis that the advancement of PC may be linked to the increased expression of EGFR and poor prognosis [23] (Fig. 1A, B). Likely, the EGFR expression rate was increased at the major stage II in PC with $p = 0.00607$ (Fig. 1C).

Analysis of EGFR expression from the TCGA database indicated its upregulation in the age groups between 41 and 80 years. However, the expression rate increased in the age group, particularly between 41 and 60 years (Fig. 1D). Most patients, over 50 years of age are diagnosed with PC, and the most common onset is between 60 and 80 years [23, 24]. Due to concomitant conditions or poor health, elderly people with PC typically have a poorer prognosis for survival than their younger counterparts [25]. Liu et al., [26] also stated that higher EGFR expression was substantially correlated with a shorter patient lifespan, necessitating the development of new therapeutic approaches for these EGFR-driven tumors [26]. Hence, we are intrigued to investigate the efficacy of plumbagin to inhibit the actions induced by EGF in human PC cell line PANC-1 cells. Our laboratory is focused to develop small molecule inhibitors for mitigating EGFR-driven cancer. Previous preliminary investigations were conducted to screen the effective lead molecule using a bioassay-guided approach involving MMP-2-identified plumbagin among eight components tested to exert better inhibitory effects in PANC-1 cells. The efficacy was assessed in terms of its ability to reduce viability and activities of MMP-2, a marker of metastasis [17]. The current study is planned to explore the efficacy of plumbagin to mitigate EGF actions in PANC-1 cells [5]. To address this objective, the efficacy of plumbagin is evaluated under basal and EGF-stimulated conditions in the present study. Herein, we showed that plumbagin dose-dependently reduces viability after 24 h of treatment. The reduction in the survival of PANC-1 cells is due to the arrest of the S phase in the cell cycle after 24 h of plumbagin treatment. Pandey et al., [27] also reported that plumbagin induced a reduction in the survival and cell cycle arrest in MIA PaCa2 and PANC-1 cells. Also, they reported that plumbagin induces apoptotic morphological changes in both cell lines tested. In the present study, we showed that plumbagin induces apoptosis after 24 h of treatment in basal and EGF-stimulated cells. EGF is a well-known mitogen that enhances cancer cell proliferation. The cells stimulated with 50 ng/ml EGF significantly increased the viability of PANC-1 cells. Interestingly, plumbagin treatment for 24 h greatly inhibits the survival of PANC-1 cells under basal and EGF-treated cells. These changes by plumbagin assume greater significance. EMT is an important event for the migration, invasion, and metastasis of several cancers including PC. These results are in agreement with an earlier

Fig. 5 The structure of EGFR (**A**). The ability of plumbagin to interact with different domains of EGFR was determined and the docked complex of plumbagin with the EGFR domains. Putative amino acids involved and the type of interactions involved are depicted (**B–E**)

report wherein plumbagin prevented EMT in PC cells [28]. Further, the present study results strengthen the therapeutic utility of plumbagin as it prevented the EGF-stimulated actions. Several studies documented the prognostic significance of blocking EGF actions to control metastasis, especially using small molecule inhibitors. Plumbagin is a small molecule with lesser molecular weight and is more effective in reducing the actions of EGF. The present findings are promising and warrant pre-clinical investigation to ascertain the toxicity and availability of plumbagin/its metabolites at the target site/circulation.

Binker et al., [29] reported that EGF-stimulated PANC-1 cells secreted a higher amount of MMP-2 via activating PI3K and Src signaling. Consistent with their findings our results also showed that increased secretion of MMP-2 was evidenced in EGF-treated PANC-1 cells. EGF-induced MMP-2 secretion was abrogated by plumbagin treatment and pre-treatment. A decrease in the activity of MMP-2 can be attributed to decreased MMP-2 gene expression and increased proteosomal degradation. Plumbagin greatly reduced the abundance of MMP-2 transcripts suggesting these effects as a consequence of impairment of transcription factor activation through disruption of EGFR signaling. Plumbagin prevents PI3K and p38 MAPK activation via inhibiting phosphorylation in PC cell lines may be responsible for this blocking of MMP-2 activities [28]. EGF is known to facilitate the migration of cancer cells by upregulating MMP-2 and mesenchymal markers. The wound healing assay is a two-dimensional method that is frequently used to assess cell migration. EGF stimulation expedited cell migration in PANC-1 cells in tune with a reported study by [30]. In the current study, we also showed that EGF-treatment induced faster healing of scratched wound areas by promoting migration. This EGF-induced migration was greatly retarded by plumbagin and this may be due to the inhibiting the activities of migratory protein MMP-2.

The colonization ability of cancer cells is mainly due to cancer stemness leading to metastasis as well as recurrence of the tumor. The anchorage-independent cancer cells developed resistance against anoikis, cell death of epithelial cells detached from ECM [31]. The potential ability of EGF to induce colony formation in the PC cell lines is reported by Li et al., [32]. The current study is emphasizing the ability of plumbagin to prevent colony formation induced by EGF as well as basal conditions. Consistent with our findings, Pandey et al., [20] documented the inhibitory action of

plumbagin in preventing colony formation in a dose-dependent manner in PC cells. Hyaluron is an important non-collagenous glycosaminoglycan commonly present in ECM. In PC and other solid malignancies, overexpression of HA is thought to be 87%, which can be linked to poor prognosis due to reduced access to drugs. The hyaluron accumulation in the stromal region has been linked to a poor prognosis and has an impact on immune surveillance in PC [33]. Our data on increased hyaluron production significantly increased in EGF-treated cells lends support to earlier arguments. This could be a result of growth factor-induced milieu activating pancreatic stellate cells to synthesize abundant hyaluron in the stroma [34]. Under basal and EGF-stimulated cells, plumbagin substantially reduces hyaluron production. This inhibition could be attributed to the blockade of hyaluron-cluster of differentiation (CD44) signal transduction by plumbagin [35]. Plumbagin strongly binds with various domains of EGFR is evidenced using molecular docking in the current study. Hafeez et al., [18] reported the inhibitory actions of plumbagin in the substantial expression of EGFR and its interaction with STAT3 in PANC-1 cells and xenograft PC tissue. The ability of plumbagin to bind with EGFR is the reason for inhibiting the EGFR expression and phosphorylation to block further signal transduction which may help to inhibit PC progression and metastasis.

Conclusion

In conclusion, our findings suggest that the EGFR increased expression rate was strongly associated with the PC patient's OS rate, elderly age, and advancement of PC stages. Our data strongly supports the ability of plumbagin to mitigate the actions of EGF in PANC-1 cells. Several hallmarks of resistance and migration due to EGF TME are effectively attenuated by plumbagin. The computational studies indicate the greater affinity of plumbagin with different domains of EGFR than gefitinib. Our study, therefore, warrants investigating the actions of plumbagin in a pre-clinical study to substantiate these findings. Plumbagin, being a component of the edible plant *Plumbago zeylanica*, consumption of this plant at indicated amount along with conventional therapy could be very effective in the management of PC. Our study also warrants studying the combined efficacy of plumbagin and gemcitabine for newer drug combinations.

Acknowledgements This study is supported by a seed money grant from the host institution (No.KAHE/R-Acad/A1/Seed Money/035/2022). The constructive periodic discussions and support headed by the Managing Director, Dr. R. Vasanthakumar, Karpagam Education Institutions are responsible for this work. The authors thank the CEO, Vice-Chancellor, and Registrar of KAHE for providing constructive support for the completion of this work.

Author contributions Conception, experimental design, and final manuscript preparation: SM. Performing the cell-based experiments and initial manuscript preparation: LP. Execution of in silico experiments: BM.

Funding KAHE, KAHE/R-Acad/A1/Seed Money/035/2022, Sridhar Muthusami.

Data availability Upon reasonable request, the data will be made available.

Declarations

Conflict of interest The authors declare no conflicts of interest.

References

- Galli R, Schmutz-Kober K, Kühnel J, Maak M, Rosenberg R. Pankreaskarzinom [Pancreatic cancer]. *Therapeutische Umschau Revue thérapeutique*. 2021;78(10):605–13. <https://doi.org/10.1024/0040-5930/a001317>.
- Pawlik TM. Pancreatic Cancer. *Surg Oncol Clin N Am*. 2021;30(4):xiii–xv. <https://doi.org/10.1016/j.soc.2021.07.002>.
- Gaidhani RH, Balasubramaniam G. An epidemiological review of pancreatic cancer with special reference to India. *Indian J Med Sci*. 2021;73(1):99–109. https://doi.org/10.25259/IJMS_92_2020.
- Shrikhande SV, Barreto S, Sirohi B, Bal M, Shrimali RK, Chacko RT, Rath GK. Indian council of medical research consensus document for the management of pancreatic cancer. *Indian J Med Paediat Oncol*. 2019;40(01):9–14. https://doi.org/10.4103/ijmpo.ijmpo_29_19.
- Muthusami S, Prabakaran DS, Yu JR, Park WY. EGF-induced expression of Fused Toes Homolog (FTS) facilitates epithelial-mesenchymal transition and promotes cell migration in ME180 cervical cancer cells. *Cancer Lett*. 2014;351(2):252–9. <https://doi.org/10.1016/j.canlet.2014.06.007>.
- Xelwa N, Candy GP, Devar J, Omoshoro-Jones J, Smith M, Nweke EE. Targeting growth factor signaling pathways in pancreatic cancer: towards inhibiting chemoresistance. *Frontiers Oncol*. 2021;11:683788. <https://doi.org/10.3389/fonc.2021.683788>.
- Xu Z, Zhang Y, Jiang J, Yang Y, Shi R, Hao B, Zhang Z, Huang Z, Kim JW, Zhang G. Epidermal growth factor induces HCCR expression via PI3K/Akt/mTOR signaling in PANC-1 pancreatic cancer cells. *BMC Cancer*. 2010;10:161. <https://doi.org/10.1186/1471-2407-10-161>.
- Fitzgerald TL, Lertpiriyapong K, Cocco L, Martelli AM, Libra M, Candido S, Montalto G, Cervello M, Steelman L, Abrams SL, McCubrey JA. Roles of EGFR and KRAS and their downstream signaling pathways in pancreatic cancer and pancreatic cancer stem cells. *Adv Bioll Regul*. 2015;59:65–81. <https://doi.org/10.1016/j.jbior.2015.06.003>.
- Park SJ, Gu MJ, Lee DS, Yun SS, Kim HJ, Choi JH. EGFR expression in pancreatic intraepithelial neoplasia and ductal adenocarcinoma. *Int J Clin Exp Pathol*. 2015;8(7):8298–304.
- Uribe ML, Marrocco I, Yarden Y. EGFR in cancer: signaling mechanisms, drugs, and acquired resistance. *Cancers*. 2021;13(11):2748. <https://doi.org/10.3390/cancers13112748>.
- Periyasamy L, Muruganatham B, Deivasigamani M, Lakshmanan H, Muthusami S. Acetogenin extracted from annona muricata prevented the actions of EGF in PA-1 ovarian cancer cells. *Protein Pept Lett*. 2021;28(3):304–14. <https://doi.org/10.2174/0929866527666200916141730>.
- Muthusami S, Sabanayagam R, Periyasamy L, Muruganatham B, Park WY. A review on the role of epidermal growth factor signaling in the development, progression, and treatment of cervical cancer. *Int J Biol Macromol*. 2022;194:179–87. <https://doi.org/10.1016/j.ijbiomac.2021.11.117>.
- Valsecchi ME, McDonald M, Brody JR, Hyslop T, Freydin B, Yeo CJ, Solomides C, Peiper SC, Witkiewicz AK. Epidermal growth factor receptor and insulinlike growth factor 1 receptor expression predict poor survival in pancreatic ductal adenocarcinoma. *Cancer*. 2012;118(14):3484–93. <https://doi.org/10.1002/cncr.26661>.
- Nedaeinia R, Avan A, Manian M, Salehi R, Ghayour-Mobarhan M. EGFR as a potential target for the treatment of pancreatic cancer: dilemma and controversies. *Curr Drug Targets*. 2014;15(14):1293–301. <https://doi.org/10.2174/1389450115666141125123003>.
- Yang ZY, Yuan JQ, Di MY, Zheng DY, Chen JZ, Ding H, Wu XY, Huang YF, Mao C, Tang JL. Gemcitabine plus erlotinib for advanced pancreatic cancer: a systematic review with meta-analysis. *PLoS ONE*. 2013;8(3):e57528d. <https://doi.org/10.1371/journal.pone.0057528>.
- Periyasamy L, Muruganatham B, Park WY, Muthusami S. Phyto-targeting the CEMIP expression as a strategy to prevent pancreatic cancer metastasis. *Curr Pharm Des*. 2022;28(11):922–46. <https://doi.org/10.2174/1381612828666220302153201>.
- Periyasamy L, Muruganatham B, Sundararaj R, Krishnamoorthy S, Muthusami S. Screening of MMP-2 inhibiting phytoconstituents for the development of newer pancreatic cancer modalities. *Protein Pept Lett*. 2023; 30(4):304–313. <https://doi.org/10.2174/0929866530666230213113835>.
- Hafeez BB, Jamal MS, Fischer JW, Mustafa A, Verma AK. Plumbagin, a plant derived natural agent inhibits the growth of pancreatic cancer cells in vitro and in vivo via targeting EGFR, Stat3 and NF-κB signaling pathways. *Int J Cancer*. 2012;131(9):2175–86. <https://doi.org/10.1002/ijc.27478>.
- Tang Z, Kang B, Li C, Chen T, Zhang Z. GEPIA2: an enhanced web server for large-scale expression profiling and interactive analysis. *Nucleic Acids Res*. 2019;47(W1):W556–60. <https://doi.org/10.1093/nar/gkz430>.
- Rappé AK, Casewit CJ, Colwell KS, Goddard WA III, Skiff WM. UFF, a full periodic table force field for molecular mechanics and molecular dynamics simulations. *J Am Chem Soc*. 1992;114(25):10024–35. <https://doi.org/10.1021/ja00051a040>.
- Trott O, Olson AJ. AutoDock Vina: improving the speed and accuracy of docking with a new scoring function, efficient optimization, and multithreading. *J Comput Chem*. 2010;31(2):455–61. <https://doi.org/10.1002/jcc.21334>.
- Dallakyan S, Olson AJ. Small-molecule library screening by docking with PyRx. *Meth Mol Biol*. 2015;1263:243–50. https://doi.org/10.1007/978-1-4939-2269-7_19.
- Sohal DP, Mangu PB, Laheru D. Metastatic pancreatic cancer: american society of clinical oncology clinical practice guideline summary. *J Oncol Pract*. 2017;13(4):261–4. <https://doi.org/10.1200/JOP.2016.017368>.
- Rawla P, Sunkara T, Gaduputi V. Epidemiology of pancreatic cancer: global trends, etiology and risk factors. *World J Oncol*. 2019;10(1):10–27. <https://doi.org/10.14740/wjon1166>.
- Macchini M, Chiaravalli M, Zanon S, Peretti U, Mazza E, Gianni L, Reni M. Chemotherapy in elderly patients with pancreatic cancer: Efficacy, feasibility and future perspectives. *Cancer Treat Rev*. 2019;72:1–6. <https://doi.org/10.1016/j.ctrv.2018.10.013>.
- Liu H, Zhang B, Sun Z. Spectrum of EGFR aberrations and potential clinical implications: insights from integrative pan-cancer analysis. *Cancer Commun*. 2020;40(1):43–59. <https://doi.org/10.1002/cac2.12005>.

27. Pandey K, Tripathi SK, Panda M, Biswal BK. Prooxidative activity of plumbagin induces apoptosis in human pancreatic ductal adenocarcinoma cells via intrinsic apoptotic pathway. *Toxicol in vitro Int J published Assoc.* 2020;65:104788. <https://doi.org/10.1016/j.tiv.2020.104788>.
28. Wang F, Wang Q, Zhou ZW, Yu SN, Pan ST, He ZX, Zhang X, Wang D, Yang YX, Yang T, Sun T, Li M, Qiu JX, Zhou SF. Plumbagin induces cell cycle arrest and autophagy and suppresses epithelial to mesenchymal transition involving PI3K/Akt/mTOR-mediated pathway in human pancreatic cancer cells. *Drug Des Dev Ther.* 2015;9:537–60. <https://doi.org/10.2147/DDDT.S73689>.
29. Binker MG, Binker-Cosen AA, Richards D, Oliver B, Cosen-Binker LI. EGF promotes invasion by PANC-1 cells through Rac1/ROS-dependent secretion and activation of MMP-2. *Biochem Biophys Res Commun.* 2009;379(2):445–50. <https://doi.org/10.1016/j.bbrc.2008.12.080>.
30. Liu W, Wang K, Gong K, Li X, Luo K. Epidermal growth factor enhances MPC-83 pancreatic cancer cell migration through the upregulation of aquaporin 3. *Mol Med Rep.* 2012;6(3):607–10. <https://doi.org/10.3892/mmr.2012.966>.
31. Taddei ML, Giannoni E, Fiaschi T, Chiarugi P. Anoikis: an emerging hallmark in health and diseases. *J Pathol.* 2012;226(2):380–93. <https://doi.org/10.1002/path.3000>.
32. Li J, Kleeff J, Giese N, Büchler MW, Korc M, Friess H. Gefitinib (“Iressa”, ZD1839), a selective epidermal growth factor receptor tyrosine kinase inhibitor, inhibits pancreatic cancer cell growth, invasion, and colony formation. *Int J Oncol.* 2004;25(1):203–10.
33. Tahkola K, Ahtiainen M, Mecklin JP, Kellokumpu I, Laukkanen J, Tammi M, Tammi R, Väyrynen JP, Böhm J. Stromal hyaluronan accumulation is associated with low immune response and poor prognosis in pancreatic cancer. *Sci Rep.* 2021;11(1):12216. <https://doi.org/10.1038/s41598-021-91796-x>.
34. Seufferlein T, Ducreux M, Hidalgo M, Prager G, Van Cutsem E. More than a gel-Hyaluronic acid, a central component in the microenvironment of pancreatic cancer. *Eur Oncol Haematol.* 2018;14(1):40–4. <https://doi.org/10.17925/EOH.2018.14.1.40>.
35. Roy R, Mandal S, Chakrabarti J, Saha P, Panda CK. Downregulation of Hyaluronic acid-CD44 signaling pathway in cervical cancer cell by natural polyphenols Plumbagin, Pongapin and Karanjin. *Mol Cell Biochem.* 2021;476(10):3701–9. <https://doi.org/10.1007/s11010-021-04195-1>.

Publisher's Note Springer Nature remains neutral with regard to jurisdictional claims in published maps and institutional affiliations.

Springer Nature or its licensor (e.g. a society or other partner) holds exclusive rights to this article under a publishing agreement with the author(s) or other rightsholder(s); author self-archiving of the accepted manuscript version of this article is solely governed by the terms of such publishing agreement and applicable law.